

## Covalency effects on the magnetism of $\text{EuRh}_2\text{P}_2$

This article has been downloaded from IOPscience. Please scroll down to see the full text article.

2008 J. Phys.: Condens. Matter 20 285229

(<http://iopscience.iop.org/0953-8984/20/28/285229>)

View [the table of contents for this issue](#), or go to the [journal homepage](#) for more

Download details:

IP Address: 129.252.86.83

The article was downloaded on 29/05/2010 at 13:33

Please note that [terms and conditions apply](#).

# Covalency effects on the magnetism of $\text{EuRh}_2\text{P}_2$

Robert Schmitz and Erwin Müller-Hartmann

Institut für Theoretische Physik, Universität zu Köln, Zùlpicher Straße 77,  
50937 Köln, Germany

Received 24 April 2008, in final form 1 June 2008

Published 24 June 2008

Online at [stacks.iop.org/JPhysCM/20/285229](http://stacks.iop.org/JPhysCM/20/285229)

## Abstract

In experiments, the ternary Eu pnictide  $\text{EuRh}_2\text{P}_2$  shows an unusual coexistence of a non-integral Eu valence of about 2.2 and a rather high Néel temperature of 50 K. In this paper, we present a model which explains the non-integral Eu valence via covalent bonding of the Eu 4f-orbitals to  $\text{P}_2$  molecular orbitals. In contrast to intermediate valence models where the hybridization with delocalized conduction band electrons is known to suppress magnetic ordering temperatures to at most a few kelvin, covalent hybridization to the localized  $\text{P}_2$  orbitals avoids this suppression. Using perturbation theory we calculate the valence, the high-temperature susceptibility, the Eu single-ion anisotropy and the superexchange couplings of nearest and next-nearest neighbouring Eu ions. The model predicts a tetragonal anisotropy of the Curie constants. We suggest an experimental investigation of this anisotropy using single crystals. From experimental values of the valence and the two Curie constants, the three free parameters of our model can be determined.

## 1. Introduction

### *Non-integral valence, intermediate valence, and magnetic order*

A general question of interest is how a non-integral valence of localized ions in a solid influences the possibility of magnetic order. Concerning this subject, an earlier paper reported the anomalous valence state of Eu in  $\text{EuRh}_2\text{P}_2$  [1].  $\text{EuRh}_2\text{P}_2$  was characterized as showing intermediate-valent and probably also covalent properties. The coexistence of a non-integral Eu valence of 2.2 and antiferromagnetic order up to 50 K was reported.

Simply given, a non-integral valence means that the mean total occupation number of the ionic electronic levels is non-integral. This might have several physical reasons. In particular, *intermediate valence* is the hybridization of localized ionic states with the strongly *delocalized* conduction band. It is experimentally evident and theoretically well understood that there is a strong competition between intermediate valence and magnetic order. Intermediate valence is known to suppress magnetic ordering temperatures typically to at most a few K. As an experimental example, TmSe is intermediate-valent and has a Néel temperature below 3.5 K [2].

A detailed theoretical approach to intermediate valence is the extended s-f model [3]. Using this model a similarity to the

Kondo effect is shown: broadly speaking, information about the electron spin is washed out by the delocalization of the conduction band states. The extended s-f model allows one to take a ferromagnetic exchange between ionic f and conducting s states into account, which is typical for intermediate-valent Eu ions. Hence, it is more realistic than an Anderson model, which always implies an antiferromagnetic s-f coupling [4].

In agreement with experiment, the extended s-f model also explains why the magnetic ordering temperature of an intermediate-valent system is enhanced drastically by mechanical or chemical high pressure. In addition, a given intermediate valence is pressure-sensitive itself because the energy levels of the localized states can be pressed towards the conduction band. These aspects are not too important for the present paper because we will concentrate neither on intermediate valence nor on anomalous pressure.

If a non-integral valence is caused by *covalence*, *no strongly delocalized states* are involved in the underlying hybridization. Hence, a characteristically different approach will be required to understand such systems.

The interpretation of  $\text{EuRh}_2\text{P}_2$  is insufficient so far. On the one hand, if  $\text{EuRh}_2\text{P}_2$  was a system in which a Eu intermediate valence of 2.2 and magnetic order coexist up to 50 K without any restrictions, this would be most surprising. Not only is such behaviour experimentally unusual but also theoretically not understood, because in this case the ordering temperature

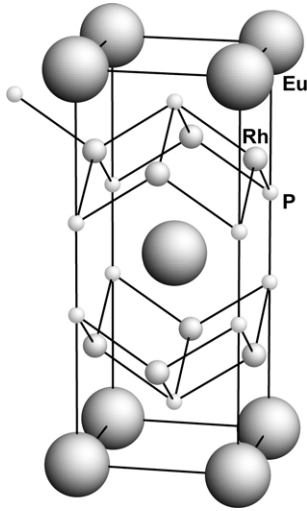


**Figure 1.** Crystal structure of  $\text{EuRh}_2\text{P}_2$ .

is an order of magnitude higher than for typically realistic parameter sets of the extended  $s$ - $f$  model [3]. Even for extreme choices of the model parameters (in case of a Eu intermediate valence of 2.2), an upper boundary of about 15 K for the ordering temperature is estimated. A new concept of intermediate valence would have to be found to explain the experiment. On the other hand, no detailed model is available to investigate the counter-perspective, the influence of the covalence on the magnetism of  $\text{EuRh}_2\text{P}_2$ .

In the following, we will motivate the use of a covalent scenario *instead* of intermediate valence as the starting point for the investigation of  $\text{EuRh}_2\text{P}_2$ . This is in contrast to former publications [1, 5–7] and also refers to unpublished experimental material [8–11].

#### *The covalence of $\text{EuRh}_2\text{P}_2$*

We take into account the following experiments on  $\text{EuRh}_2\text{P}_2$ : measurements of the magnetic susceptibility [1, 9], of the crystal structure [5, 7, 11],  $L_{\text{III}}$  x-ray absorption [8], and Mössbauer spectroscopy [10].

The properties of  $\text{EuRh}_2\text{P}_2$  can be unravelled by studying the influences of temperature and doping, especially with As. Depending on these two parameters, in experiments a structural phase transition of first order is observed whilst the lattice type, a body-centred tetragonal  $\text{ThCr}_2\text{Si}_2$  structure (figure 1), does not change.

The structural phases  $\alpha$  and  $\beta$  differ by a strongly anisotropic jump of the lattice parameters and in the electronic bonding conditions. This leads in the  $\beta$  phase to a non-integral Eu valence of 2.2. The lattice cells show a slight elongation in the square plane but a considerable compression along the tetragonal axis [5, 7, 11] compared to the  $\alpha$  phase, which contains divalent Eu ions. In both phases, the valence is homogeneous, i.e., all Eu ions are equivalent.

In the  $\beta$  modification two nearest neighbouring P atoms form a single molecular bond [7, 11]—oriented along the tetragonal axis—which does not appear in the  $\alpha$  phase. This corresponds to a charge transfer from the phosphorus to the

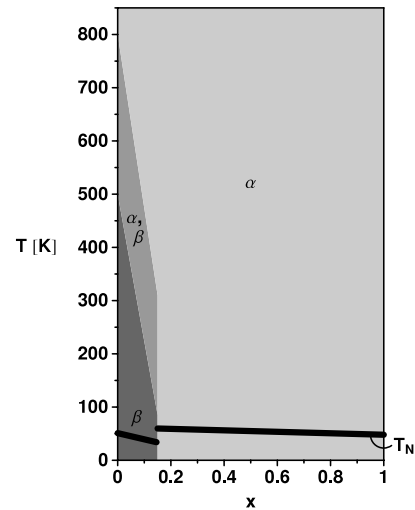


**Figure 2.** Phase diagram of  $\text{EuRh}_2(\text{As}_x\text{P}_{1-x})_2$  [9]. The mid-grey sector corresponds to a coexistence due to hysteresis.

conduction band, which leaves holes in  $\text{P}_2$  molecular states. These are available for occupation by one fluctuating Eu electron each. In this way, in the  $\beta$  phase there is a covalent hybridization between the magnetic Eu ions and  $\text{P}_2$  molecules. The Rh ions do not participate in the magnetic properties of  $\text{EuRh}_2\text{P}_2$ .

Both phases  $\alpha$  and  $\beta$  exhibit a magnetic phase transition from para- to antiferromagnetism at a Néel temperature  $T_N$  (phase diagram: figure 2). With decreasing As doping  $T_N$  drops somewhat at the  $\alpha$ - $\beta$  phase boundary but does not change its order of magnitude. According to the extended  $s$ - $f$  model this effect of the valence transition on the ordering temperature is too small to be consistent with intermediate valence.

The valence measurements on  $\text{EuRh}_2\text{P}_2$ , in particular  $L_{\text{III}}$  x-ray absorption and Mössbauer spectroscopy, cannot distinguish between a non-integral valence of covalent and intermediate-valent origin. The reduced magnetic moment of the  $\beta$  phase compared to the divalent Eu moment of the  $\alpha$  phase does not clarify the nature of the non-integral valence either. Furthermore, the valence cannot be derived from the magnetic Eu moment alone because in the non-intermediate-valent case a non-trivial contribution by the  $\text{P}_2$  states must be considered. This quantity is unknown.

The covalent bonding scenario between Eu and  $\text{P}_2$  states pursued in the present paper was derived in [11] from bonding lengths and is supported by further aspects. In particular, the pressure dependence [10] of the valence, which we express as the deviation  $\Delta W$  from the divalent state, leads to the conclusion that the intermediate-valent part of the total Eu valence amounts to at most

$$\Delta W|_{\text{iv}} \approx 0.05. \quad (1)$$

This is the precision with which the Eu valence is determined by Mössbauer spectroscopy [10]. Reference [10] states *no* intermediate valence within this precision because in Mössbauer spectroscopy the Eu valence does not change over the range between ambient pressure and 5 GPa. This is the expectation in the absence of a conduction band hybridization.

As the results of  $L_{\text{III}}$  x-ray absorption [8] may be influenced by final-state effects, we assume an error bar for the non-integral Eu valence of the  $\beta$  phase including intermediate valence as well as covalence and estimate the valence shift as:

$$\Delta W = 0.20 \pm 0.05. \quad (2)$$

We will not carry out an error calculation in closed form but will select several discrete values for parameters of the model, which will be constituted neglecting  $\Delta W_{\text{iv}}$ . Furthermore, we ignore the weak temperature dependence of the valence which is considerably less significant in the  $\beta$  phase than the precision of 0.05 [10].

The mechanism and the geometric structure of *magnetic ordering* in  $\text{EuRh}_2\text{P}_2$  are almost completely unknown. Experimentally, antiferromagnetism below  $T_{\text{N}}$  has been concluded, as well as the existence of—unspecified—ferromagnetic couplings because of an anomalous paramagnetic Curie temperature [9]. In addition, the importance of a phosphorus-mediated superexchange between the Eu ions has been shown qualitatively via the sensitivity of the Mössbauer magnetic hyperfine field (and  $T_{\text{N}}$ ) to pressure [10], which is not observed in the reference system  $\text{EuRh}_2\text{As}_2$ .

We conclude that the covalence of  $\text{EuRh}_2\text{P}_2$  has to be significant because the intermediate-valent part is small and the reduced magnetic moment, the existence of the superexchange, and the bonding scenario have been shown to be mutually consistent with the covalence.

Any possibility other than covalence or intermediate valence which can cause a measured non-integral valence should be excluded in  $\text{EuRh}_2\text{P}_2$ : In  $\text{Eu}(\text{Pd}_{0.7}\text{Au}_{0.3})_2\text{Si}_2$  similar  $L_{\text{III}}$  x-ray absorption and Mössbauer results in spite of a *divalent* magnetic Eu moment are found at ambient pressure and are explained finally by an anomalous spatial extension of the 4f shell, whereas the system becomes intermediate-valent under high pressure [12]. In contrast to  $\text{EuRh}_2\text{P}_2$ , in  $\text{Eu}(\text{Pd}_{0.7}\text{Au}_{0.3})_2\text{Si}_2$  no covalent bonding partners are available for the Eu ions.

Under pressure beyond 5 GPa, intermediate valence in  $\text{EuRh}_2\text{P}_2$  acquires, at least qualitatively, the same relevance as the covalence but remains less important than the latter at ambient pressure [10]. The corresponding characteristic decrease of  $T_{\text{N}}$  under increasing pressure is understood by the extended s–f model.

Band structure calculations of  $\text{EuRh}_2\text{P}_2$  have only been performed for the integral-valent  $\alpha$  (high-temperature) phase [6].

The magnetic ordering of  $\text{EuRh}_2\text{P}_2$  is caused both by super and indirect exchange. The latter aspect follows because the reference system  $\text{EuRh}_2\text{As}_2$  exhibits almost the same  $T_{\text{N}}$  (48 K) but neither superexchange [10] nor an anomaly of the paramagnetic Curie temperature [9].

In order to treat the covalence effects of  $\text{EuRh}_2\text{P}_2$  perturbatively from divalent ionic ground states, we view the crystal as built by inactive two-dimensional metallic Rh planes and by quasi-two-dimensional insulating  $\text{EuP}_2$  planes. The covalent hybridization in these planes is much more important than the one between different  $\text{EuP}_2$  planes. This is concluded from the Eu–P distances, which in the  $\beta$  phase near the phase

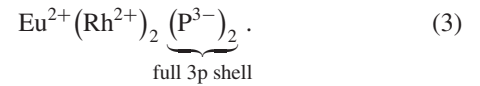
boundary are: 3.88 Å between the planes and 3.10 Å in the plane.

As the starting point we view the properties of an arbitrary single Eu ion in interaction with the four neighbouring  $\text{P}_2$  molecular ions which form a tetragonal cage around it. This interaction describes the high-temperature paramagnetism of the crystal to leading order. We begin with three unknown model parameters and reduce their number finally to one after calculating two quantities for which experimental values are available: the valence and the paramagnetic susceptibility (as an average over the three spatial directions). We also calculate the single-ion anisotropies of the Eu ions, which are experimentally unknown.

Using the same model parameters, since thermal expansion is very small in the temperature range between 0 and about 400 K [7], we calculate the superexchange parameters between nearest and next-nearest neighbouring Eu ions.

## 2. Model

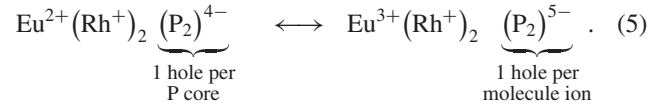
The  $\alpha$  phase of  $\text{EuRh}_2\text{P}_2$  has got the formal valences [11]:



This corresponds to the divalent ground state of a Eu ion:

$$4f^7, \quad S = \frac{7}{2}, \quad L = 0, \quad J = S. \quad (4)$$

In the covalent  $\beta$  phase there is a fluctuation between the formal valences [11]:



The hybridization of the Eu ions is described perturbatively—starting from the divalent configuration—via a quantum mechanical admixture of trivalent states:

$$4f^6, \quad S = 3, \quad L = 3, \quad J = 0 \dots 6. \quad (6)$$

Hund’s rule correlations are taken fully into account. We use a Landé approximation for the energies  $E_J$  of the  $\text{Eu}^{3+}$  ground state  $J = 0$  and the low excitations  $J > 0$ :

$$E_J = \Delta E [1 + XJ(J + 1)]. \quad (7)$$

$E_{J=0}$  is shifted by an unknown charge transfer energy  $\Delta E$  with respect to the divalent ground state, which is the zero point in our calculation ( $E_{2+} = 0$ ). The intraionic spin–orbit part of the levels  $E_J$  is given by

$$X = \frac{\xi}{42\Delta E}, \quad \xi = 7960 \text{ K} \quad (8)$$

which was fitted to optical measurements [13] by a least squares fit.  $\xi$  is the spin–orbit coupling parameter ( $H_{\text{so}} = \xi \mathbf{LS}$

is the Hamiltonian of the spin–orbit coupling for a single Eu ion).

After an electron hops from the Eu ion to a phosphorus ion, it occupies an antibonding molecular orbital (MO) state, which is considered as a linear combination of two  $3p_z$  atomic orbitals due to the MO method and which is odd under a reflection with respect to the  $a^2(xy)$  plane. The bonding  $3p_z$  MOs are always filled.

As the perturbation term which expresses the covalent hybridization we introduce a hopping operator between a Eu ion and four neighbouring  $P_2$  molecular ions:

$$V = \sum_{\substack{k=1,2,3,4 \\ \sigma=\uparrow,\downarrow}} [t_0 f_{0\sigma}^\dagger + (-1)^k t_2 (f_{-2\sigma}^\dagger + f_{2\sigma}^\dagger)] p_\sigma^{(k)} + \text{H.c.} \quad (9)$$

$p$  and  $f$  denote the annihilators corresponding to the single-particle states. Because of symmetries (time reversal of the crystal Hamiltonian, reflection with respect to  $xy$  and  $xz$  plane) contributions due to hopping amplitudes  $t_m$  for magnetic quantum numbers  $m \neq 0, \pm 2$  are excluded and we have  $t_{-2} = t_2$ .  $p_\sigma^{(k)}$  relates to the antibonding MO of the  $k$ th neighbour. There are three unknown model parameters:  $X$ ,  $t_0$ , and  $t_2$ . The hopping amplitudes can be chosen real.

We calculate the matrix elements of effective operators via standard perturbation theory for a degenerate system and to leading order in the perturbation. We use a formulation due to Takahashi [14] involving a unitary transformation  $\Gamma$  which maps the perturbed problem onto the unperturbed ground-state space.  $\Gamma$  is given as a power series in terms of the unperturbed Hamiltonian—corresponding here to the energies  $E_{2+} = 0$  and  $E_J$ —and the perturbation operator  $V$ . Any operator  $A$  in the Hilbert space of the perturbed states is treated as an effective operator  $a = \Gamma^\dagger A \Gamma$  in the ground-state space.

In the calculation, the matrix elements of the effective operators are expressed in terms of the matrix elements of the  $f$  creators (which appear in the perturbation term  $V$ ) between the correlated many-body states of the  $\text{Eu}^{2+}$  and  $\text{Eu}^{3+}$  ions. The matrix elements are evaluated via Clebsch–Gordan coefficients and the Wigner–Eckart theorem. Explicitly, using Clebsch–Gordan coefficients the  $f$  creators are transformed from the  $m\sigma$  to the  $j j_z$  basis:

$$f_{m\sigma}^\dagger = \sum_{\substack{j=\frac{5}{2}, \frac{7}{2} \\ j_z=m+\sigma}} \langle 3m \frac{1}{2} \sigma | j j_z \rangle f_{j j_z}^\dagger. \quad (10)$$

The Wigner–Eckart theorem gives:

$$\langle \frac{7}{2} M | f_{j j_z}^\dagger | J J_z \rangle = \| f \|_{j J} \langle J J_z j j_z | \frac{7}{2} M \rangle, \quad (11)$$

where  $|\frac{7}{2} M\rangle$  is a state of the  $\text{Eu}^{2+}$  configuration ( $M = -7/2 \dots 7/2$ ),  $|J J_z\rangle$  is a state of the  $\text{Eu}^{3+}$  configuration ( $J = 0 \dots 6$ ,  $J_z = -J \dots J$ ), and  $\| f \|_{j J}$  is a reduced matrix element.

### 3. Single-ion effects

We calculate the matrix elements of the effective operators of the valence and the magnetization due to hopping of second

order in  $V$ , which is the leading order of the hybridization for the single-ion effects. For this calculation it is sufficient to apply the unitary operator  $\Gamma$  to first order.

We have calculated the effective single-ion Hamiltonian to second order in  $V$ . According to this calculation, which we do not present in detail, the octets of the unperturbed  $\text{Eu}^{2+}$  ions split into four Kramers doublets which, however, remain quasi-degenerate, i.e. the splitting of these doublets is very small compared to the temperature. Hence, we will use the average energy of the Kramers doublets for thermodynamic averaging.

#### Effective valence

The covalent admixture of  $\text{Eu}^{3+}$  states shifts the valence from 2 to a larger value. In order to calculate the model valence we use the valence operator:

$$W = 3 - P_0. \quad (12)$$

$P_0$  is the projector onto the unperturbed ground-state space [14]. In the framework of our perturbation method [14] we use the effective valence operator  $w = \Gamma^\dagger W \Gamma$  to second order in  $V$ . Thermodynamic averaging due to the mean eigenvalues of the effective Hamiltonian of second order gives the mean valence:

$$\langle W \rangle = \frac{1}{8} \text{tr } w. \quad (13)$$

Our calculation of the deviation  $\Delta W = \langle W \rangle - 2$  from the divalent Eu configuration caused by the covalence gives the result:

$$\Delta W = \frac{4}{49} \frac{t_0^2 + 2t_2^2}{(\Delta E)^2} \sum_{J=0}^6 \frac{1 + 2J}{[1 + J(J+1)X]^2}. \quad (14)$$

Because of the uncertainty of the precise value of  $\Delta W$  (see (1) and (2)) we carry out the model calculation using the experimental values

$$\Delta W = 0.2 \quad \text{and} \quad \Delta W = 0.15. \quad (15)$$

Fixing the value of  $\Delta W$  accordingly reduces the number of unknown model parameters from three to two. For convenience, we define

$$t = \sqrt{t_0^2 + 2t_2^2} \quad (16)$$

as the total hopping amplitude. Because of  $t_{-2} = t_2$ ,  $t^2$  is proportional to the total hopping probability of all single-particle Eu states  $m$  involved in the hopping. In view of equation (14),  $t$  can be considered a function of  $X$  at a given value of  $\Delta W$ .

In order to ensure that the second-order calculation be consistent,  $(t/\Delta E)^2$  must be considerably lower than 1. This will be the case for our choices of the model parameters. Higher orders will be suppressed by an additional factor of  $(t/\Delta E)^2$ .

### Effective Curie susceptibility

Due to the covalent admixture of the  $\text{Eu}^{3+}$  configuration the paramagnetic susceptibility of  $\text{EuRh}_2\text{P}_2$  can be expected to become anisotropic. According to the space group the susceptibility tensor has tetragonal symmetry. In the high-temperature regime we are considering here the susceptibility is Curie-like. In the limit of small differences between the energies of the Kramers doublets, the paramagnetic susceptibility of the system per space direction  $i = x, y, z$  is given by:

$$\chi_{ii} = \frac{1}{kT} C_{ii}, \quad C_{ii} = \frac{1}{8} \sum_{MM'} \left| \left\langle \frac{7}{2} M | m_i | \frac{7}{2} M' \right\rangle \right|^2, \quad (17)$$

following from the standard formula for the Curie susceptibility of single ions [15]. The Curie constants  $C_{ii}$  of second order depend on the effective magnetic moment  $m_i = \Gamma^\dagger M_i \Gamma$  of second order in  $V$ , where  $M_i = J_i + S_i$  denotes the untransformed moment. Experimentally, the Curie susceptibility has been measured on polycrystals [1, 9]. This corresponds to the spatial average  $C = (2C_{xx} + C_{zz})/3$ , and we define

$$\Delta C_{ii} = C_{ii} - C \quad (\text{implying } \Delta C_{xx} = -\frac{1}{2} \Delta C_{zz}). \quad (18)$$

The resulting model Curie constants are (in units of  $\mu_B^2$ ):

$$\begin{aligned} C = 21 - \frac{9}{49} \left( \frac{t}{\Delta E} \right)^2 & \left[ 16 + \frac{1}{1+2X} + \frac{5}{1+6X} \right. \\ & + \frac{14}{1+12X} + \frac{30}{1+20X} + \frac{55}{1+30X} + \frac{91}{1+42X} \\ & + \frac{45}{(1+2X)^2} + \frac{65}{(1+6X)^2} + \frac{70}{(1+12X)^2} \\ & \left. + \frac{54}{(1+20X)^2} + \frac{11}{(1+30X)^2} - \frac{65}{(1+42X)^2} \right], \quad (19) \\ \Delta C_{zz} = \frac{6}{49} \left( \frac{t_0}{\Delta E} \right)^2 & \left[ 24 + \frac{6}{1+2X} + \frac{26}{1+6X} + \frac{56}{1+12X} \right. \\ & + \frac{72}{1+20X} + \frac{22}{1+30X} - \frac{182}{1+42X} \\ & + \frac{63}{(1+2X)^2} + \frac{77}{(1+6X)^2} + \frac{56}{(1+12X)^2} \\ & \left. - \frac{77}{(1+30X)^2} - \frac{143}{(1+42X)^2} \right]. \end{aligned}$$

In this calculation we have included (in contrast to an intermediate-valent hybridization) non-trivial contributions to the Curie susceptibility from the localized  $p_z$  orbitals:

$$C = C^{\text{Eu}} + C^{p_z}, \quad C^{p_z} = 6\Delta W. \quad (20)$$

As  $t/\Delta E$  can be expressed via  $X$  (see equation (14)), using equations (14) and (19) we can fix  $t$  and  $X$  (and consequently,  $\Delta E$ ) from the experimental values of  $\Delta W$  and  $C$ . Similarly to the valence, we choose two experimental values of the Curie constants of the polycrystalline samples [9]:

$$C = 17.2 \quad \text{and} \quad C = 17.6. \quad (21)$$

**Table 1.** Selected sets of model parameters and maximum Curie anisotropy.

$\Delta W$	$C$	$X$	$\Delta E$	$t$	$C_{zz}^{\text{max}}/C_{xx}^{\text{min}}$
0.2	17.2	0.00181	104 687 K	24 402 K	1.018
0.15	17.6	0.009 89	19 163 K	4 505 K	1.065
0.15	17.2	0.0177	11 083 K	2 915 K	1.109

These values refer to two different samples. The latter value of  $C$  is inconsistent with  $\Delta W = 0.2$  according to the model. Probably this is not an objection to the model but a further hint at  $\Delta W < 0.2$  as far as the valence shift is caused by the covalence. We fix three sets of model parameters  $X$  (or  $\Delta E$ ) and  $t$  according to table 1. Notice that the perturbation parameter  $(t/\Delta E)^2$  is considerably lower than 1 (we have  $0.05 < (t/\Delta E)^2 < 0.07$  for all three parameter sets), which shows that the low-order calculation is sufficient. The first parameter set is the least realistic one because  $t$  is extremely high.

Table 1 shows that for a given value of  $\Delta W$ , the total hopping amplitude  $t$  is very sensitive to the value of  $C$ . Hence, it is important to take into account the contributions  $C^{p_z}$  from the  $\text{P}_2$  molecules to the paramagnetic susceptibility, see equation (20).

For convenience we define the relative hopping amplitude concerning  $m = 0$  single-particle states:

$$\tau = \frac{t_0}{t}. \quad (22)$$

After  $t$  and  $X$  (and  $\Delta E$ ) have been fixed using the experimental values of  $\Delta W$  and  $C$ ,  $\tau$  is the only unknown parameter of the model. Notice that the *anisotropy of the Curie constant*,  $\Delta C_{zz}$ , is proportional to  $\tau^2$  (see equation (19)), i.e., this anisotropy is solely caused by the covalent hybridization which involves  $m = 0$  single-particle states of the Eu-f shell.

Our model characterizes intervals (upper bounds) for the anisotropy of the Curie constant.  $C_{zz}/C_{xx} - 1 (\geq 0)$  is almost exactly proportional to  $\tau^2$ . Table 1 lists the maximum anisotropy due to:

$$C_{zz}^{\text{max}} = C_{zz}|_{\tau=1}, \quad C_{xx}^{\text{min}} = C_{xx}|_{\tau=1}. \quad (23)$$

### Single-ion anisotropy

The effective Hamiltonian to second order in the perturbation  $V$  gives rise to a single-ion anisotropy of the Eu ion:

$$h_{\text{si}} = \mu \sigma_z^2. \quad (24)$$

Here and in the following we normalize every spin operator with respect to 1 as  $\sigma_\bullet = 2S_\bullet/7$ . The single-ion anisotropy parameter  $\mu$  is given in table 2. The anisotropy changes sign for small values of  $\tau$ . We will come back to the single-ion anisotropy in the next section when we discuss various effects on the magnetic ordering temperature, which are present in  $\text{EuRh}_2\text{P}_2$ .

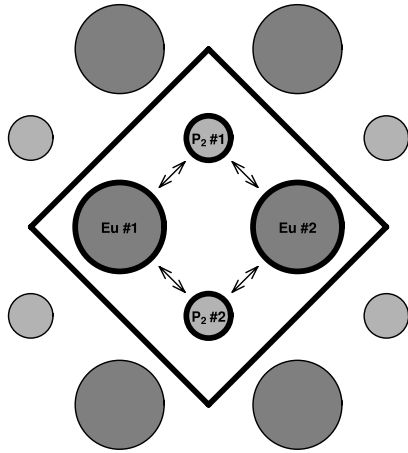


**Figure 3.** Quasi-two-dimensional  $\text{EuP}_2$  plane with a superexchange cluster of nearest neighbouring Eu ions and their common  $\text{P}_2$  molecular neighbours.

**Table 2.** Single-ion anisotropy parameter.

$X$	$\mu$ (K)
0.001 81	$14 \tau^2$
0.009 89	$-1 + 51 \tau^2$
0.0177	$-4 + 87 \tau^2$

#### 4. The coupling of neighbouring Eu spins

##### Nearest neighbours

The superexchange dynamics of nearest neighbouring Eu spins in  $\text{EuRh}_2\text{P}_2$  is described to leading order by processes of fourth order in the  $\text{Eu}-\text{P}_2$  hopping within a cluster as shown in figure 3.

In treating the intermediate states of the perturbation series, we use the same Landé levels as in section 2 and ignore Coulomb repulsion within the  $\text{P}_2$  molecules in the case of doubly occupied  $\text{P}_2$  orbitals. In analogy to equation (9), the hybridization operator is given by:

$$V = \sum_{\substack{i,k=1,2 \\ \sigma=\uparrow,\downarrow}} \left\{ t_0 f_{0\sigma}^{(i)\dagger} + (-1)^k t_2 [f_{-2\sigma}^{(i)\dagger} + f_{2\sigma}^{(i)\dagger}] \right\} p_{\sigma}^{(k)} + \text{H.c.} \quad (25)$$

$i$  is a site index for the Eu ions. We calculate the effective superexchange Hamiltonian of fourth order in  $V$  which scales with  $t^4(\Delta E)^{-3}$  and describes any superexchange in the crystal to leading order. Superexchange processes between nearest neighbouring Eu ions mediated by hopping paths exceeding the cluster we consider are at least of the order  $t^6(\Delta E)^{-5}$ .

We express the matrix elements of the effective superexchange Hamiltonian in terms of the same quantities as in section 2. The result is a finite polynomial in terms of spin operators. To a good approximation the superexchange Hamiltonian turns out as an  $xxz$  model:

$$h_{xxz} = j_x(\sigma_{1x}\sigma_{2x} + \sigma_{1y}\sigma_{2y}) + j_z \sigma_{1z}\sigma_{2z}. \quad (26)$$

There are additional (multilinear, see below) parts of the superexchange Hamiltonian, e.g., terms  $\sigma_{1i}^2\sigma_{2i}^2$ , whereas

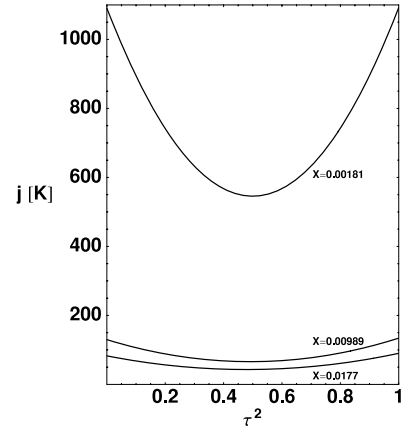


**Figure 4.** Average coupling constant of nearest neighbours.

**Table 3.** Anisotropic coupling constants of nearest neighbours.

$X$	$j_x$ (K)	$j_z$ (K)
0.001 81	$1091\tau^4 + 1091(1 - \tau^2)^2$	$1094\tau^4 + 1091(1 - \tau^2)^2$
0.009 89	$133\tau^4 + 130(1 - \tau^2)^2$	$136\tau^4 + 130(1 - \tau^2)^2$
0.0177	$89\tau^4 + 83(1 - \tau^2)^2$	$94\tau^4 + 83(1 - \tau^2)^2$

the tetragonal symmetry of the superexchange Hamiltonian is exact due to the crystal symmetry. The hopping processes we consider have got complicated selection rules. For instance, exchange processes of fourth order in  $V$  are possible where the  $z$  component of one Eu spin is changed from  $-3/2$  to  $7/2$ , i.e., these processes have the selection rule  $\Delta S_z = 5$ . This is why the exchange Hamiltonian is not bilinear in the spin operators but multilinear. For a bilinear exchange Hamiltonian the selection rule  $\Delta S_z = \pm 1$  is required. However, the exchange Hamiltonian we obtain is bilinear to a good approximation. The values of the coefficients of the neglected part of the Hamiltonian depend on the choice of the parameter sets: less than  $10^{-3}j_x$ ,  $5 \times 10^{-2}j_x$ , and  $10^{-1}j_x$  for  $X = 0.001 81$ ,  $0.009 89$ , and  $0.0177$ , respectively.

The—antiferromagnetic—coupling constants are listed in terms of *approximate* numbers in table 3. The precision of these numbers decreases with increasing value of  $X$  as the neglected parts of the Hamiltonian become more important. The lower the values of  $X$  and  $\tau$ , the more isotropic is the  $xxz$  coupling. The contribution, which is proportional to  $t_0^2 t_2^2$ , is negligible for every parameter set. Figure 4 shows the coupling, which has a considerable strength in each case, in terms of the spatial average  $j = (2j_x + j_z)/3$ .

##### Next-nearest neighbours

The calculation of the coupling of next-nearest neighbours (these are located within the  $\text{EuP}_2$  planes) is carried out using almost the same formalism as for nearest neighbours. The only difference is the single  $\text{P}_2$  molecule ion involved in this case.

The resulting superexchange Hamiltonian for next-nearest neighbours is denoted by:

$$h'_{xxz} = j'_x(\sigma_{1x}\sigma_{2x} + \sigma_{1y}\sigma_{2y}) + j'_z \sigma_{1z}\sigma_{2z}. \quad (27)$$

**Table 4.** Coupling constants of next-nearest neighbours.

$X$	$j'_x$ (K)	$j'_z$ (K)
0.001 81	273	$273\tau^4 + 273(1 - \tau^2)^2$
0.009 89	33	$32\tau^4 + 34(1 - \tau^2)^2$
0.0177	22	$21\tau^4 + 23(1 - \tau^2)^2$

The calculated coupling constants are listed in table 4. In contrast to  $h_{xxz}$ , now the  $xx$  part  $j'_x$  of the coupling is approximately independent of  $\tau$  whereas the Ising part  $j'_z$  is lower than  $j_z$  exactly by a factor of four.

#### Competing effects on the magnetic ordering temperature

As the value of the model parameter  $\tau$ , the coupling between different  $\text{EuP}_2$  planes and the effect of the indirect exchange (mediated by delocalized conduction band electrons) on the intraplanar spin couplings are not known, we cannot present a quantitative calculation of the magnetic ordering temperature. However, in the following we will argue why the considerable value of 50 K for the ordering temperature is *generic* in the framework of our model.

There are competing effects on the magnetic ordering temperature of  $\text{EuRh}_2\text{P}_2$ . (i) There is a twofold frustration of the magnetic interactions caused by the antiferromagnetic next-nearest neighbour couplings in the  $\text{EuP}_2$  planes and by the coupling between different  $\text{EuP}_2$  planes irrespective of the sign of the Heisenberg coupling  $j_{\text{inter}}$  between Eu ions in different planes, see figure 5. The frustration tends to *decrease* the magnetic ordering temperature [16]. (ii) On the other hand, there may be effects that tend to *enhance* the ordering temperature. Except for certain small values of  $\tau$ , one of these effects is the single-ion anisotropy (described by the parameter  $\mu$ , see equation (24) and table 2), which may have considerable strength compared to the superexchange couplings and may be more relevant than the  $xxz$  anisotropies of these couplings. The ordering temperature is enhanced drastically, i.e., logarithmically by a single-ion anisotropy [17]. The unknown Heisenberg exchange coupling  $j_{\text{inter}}$  or an unknown dipolar interaction between different  $\text{EuP}_2$  planes has—on the mean-field level—no effect on the ordering temperature as a hypothetically given Néel order in one plane would not cause a mean field on a Eu site in a neighbouring plane. However, the unknown anisotropies of the interplanar exchange and pseudodipolar couplings between neighbouring planes tend to stabilize the magnetic order [18].

#### Ordering temperature of an isolated quasi-two-dimensional $\text{EuP}_2$ plane

Though quantitative estimates of various magnetic couplings which may have effects on the magnetic ordering temperature as discussed above are missing, we can present estimates for that temperature according to the coupling in the quasi-two-dimensional  $\text{EuP}_2$  planes. This can serve as the *starting point* for a more comprehensive analysis in the future, in particular including the interplanar couplings which are not known to date.

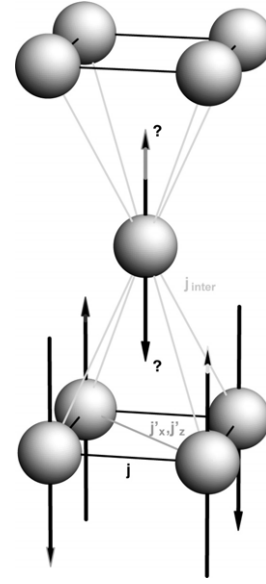


**Figure 5.** The frustration of the Eu lattice, caused by antiferromagnetic intraplanar Heisenberg couplings  $j$ . An example of four antiferromagnetically ordered spins in a  $\text{EuP}_2$  plane is shown. (i) There is a frustration caused by the antiferromagnetic next-nearest neighbour couplings  $j'_x$  and  $j'_z$  within a  $\text{EuP}_2$  plane. (ii) A nearest neighbour belonging to a different plane is geometrically frustrated independently of the sign of  $j_{\text{inter}}$ .

Reference [17] takes into account the isotropic Heisenberg couplings  $j$  of nearest neighbour magnetic ions on a two-dimensional square lattice as well as the single-ion anisotropies  $\mu$ , and estimates the magnetic ordering temperature based on these two parameters for  $\mu \ll j$ :

$$T_N = \frac{12j}{|\ln|\frac{\mu}{j}||}. \quad (28)$$

This equation gives already considerable ordering temperatures except for very narrow windows of our unknown model parameter  $\tau$ , namely  $T_N > 200$  K except for  $\tau \lesssim 10^{-12}$ ,  $0.13 \lesssim \tau \lesssim 0.15$  and  $0.21 \lesssim \tau \lesssim 0.22$  for the model parameter sets with  $X = 0.001\,81$ ,  $0.009\,89$  and  $0.0177$ , respectively.

Altogether the discussion of the competing effects on the ordering temperature and of the intraplanar estimate (28) shows that the experimentally observed ordering temperature of about 50 K is consistent with our calculations because in this sense our model avoids the suppression of the ordering temperature which is implied by intermediate-valent models [3].

#### More on interplanar exchange couplings and geometrical frustration

As mentioned above, the estimate (28) for the magnetic ordering temperature of an isolated  $\text{EuP}_2$  plane can be the starting point or *leading-order* term for a comprehensive theoretical analysis of the ordering temperature of the three-dimensional system  $\text{EuRh}_2\text{P}_2$  which we suggest should be done in the future. In particular, we expect corrections of



that first estimate according to two effects, namely (A) the *intraplanar* frustration according to the antiferromagnetic next-nearest neighbour couplings and (B) the *interplanar* frustration according to the coupling  $j_{\text{inter}}$ , which is caused by the hybridization between the  $\text{EuP}_2$  planes and the metallic Rh planes and means an effective indirect exchange coupling between the  $\text{EuP}_2$  planes.

One may *guess* that  $j_{\text{inter}}$  is ferromagnetic because [9] concludes that there are ferromagnetic couplings in the system (see section 1 above) and the intraplanar couplings are antiferromagnetic for nearest and next-nearest neighbouring Eu ions according to our calculations. However, more detailed estimates for the interplanar indirect exchange couplings including their anisotropies are going to be the subject of future theoretical work.

Once more is known about the interplanar exchange it may be promising to analyse the geometrical frustration effects on the magnetic ordering temperature. We are not aware of any reference which has discussed the twofold geometrical frustration of a tetragonal (or cubic) body-centred lattice of magnetic ions which we have identified in  $\text{EuRh}_2\text{P}_2$  with intraplanar next-nearest neighbour frustration. However, there exist several references which develop methods going beyond the estimate (28) and which may be useful for a future theoretical analysis of the magnetic ordering mechanism of  $\text{EuRh}_2\text{P}_2$ . These references analyse the low-temperature properties of various frustrated geometries for macroscopic lattices [19–22], in particular the two-dimensional square lattice with crossings as we have in the  $\text{EuP}_2$  planes [19], and investigate the possibilities of understanding frustrated systems from the properties of their building blocks which consist of small magnetic clusters [23–26]. The building blocks of the Eu lattice in  $\text{EuRh}_2\text{P}_2$  are pyramids with crossings in the basal planes.

## 5. Summary

We have introduced a systematic interpretation of the Eu valence shift and the magnetism of  $\text{EuRh}_2\text{P}_2$  due to covalent bonding which—in contrast to a hypothetically given intermediate valence—is consistent with experiment. We have presented a model for the covalence which predicts upper bounds of the anisotropy of the Curie constants and which characterizes the strength of the Eu single-ion anisotropies and of the superexchange coupling between nearest and next-nearest neighbouring Eu ions. Though a quantitative calculation of the magnetic ordering temperature has not been possible, we have argued why the experimentally observed ordering temperature is generic, because for instance the single-ion anisotropies might have considerable strength.

Measurements of the anisotropy of the Curie constants could fix the last free parameter  $\tau$  of the single-ion anisotropy and superexchange model and determine the model completely. Following that, measurements of the magnetic structure and the magnetic excitations via neutron scattering

could make a description possible which also takes into account indirect exchange between the Eu ions. (The reader should be reminded that neutron scattering requires the particularly expensive isotope Eu-153 because the standard isotope Eu-151 absorbs neutrons too strongly [2].)

A complementary possibility to fix the parameter  $\tau$  could be a numerical tight-binding fit simulation. Together with an experimental value of the anisotropy of the Curie constants, this would also mean a further consistency check of our model calculations. In order to obtain more quantitative estimates for the magnetic ordering temperature, we also suggest further theoretical work on the modelling of the interplanar indirect exchange and the consequences of the twofold (intra- and interplanar) geometrical frustration, which we have identified in the system.

In these ways, there is the chance to understand comprehensively the magnetic ordering mechanism in  $\text{EuRh}_2\text{P}_2$ .

## Acknowledgments

We thank M M Abd-Elmeguid and A Aharony for helpful discussions. This work was partially supported by the German-Israeli Foundation for Scientific Research and Development (GIF).

## References

- [1] Michels G *et al* 1996 *J. Phys.: Condens. Matter* **8** 4055
- [2] Holland-Moritz E 1983 *J. Magn. Magn. Mater.* **38** 253
- [3] Stratkötter A and Nolting W 1987 *J. Phys. C: Solid State Phys.* **20** 1103
- [4] Schrieffer J R and Wolff P A 1966 *Phys. Rev.* **140** 491
- [5] Wurth A *et al* 1997 *Z. Anorg. Allg. Chem.* **623** 1418
- [6] Johrendt D *et al* 1997 *J. Solid State Chem.* **130** 254
- [7] Huhnt C *et al* 1997 *Physica B* **240** 26
- [8] Niemöller T 1996 *Diploma Thesis* Universität zu Köln
- [9] Schütte N 1997 *Diploma Thesis* Universität zu Köln
- [10] Chefki M 1998 *Doctoral Thesis* Universität zu Köln (Aachen: Shaker)
- [11] Huhnt C 1998 *Doctoral Thesis* Universität zu Köln (Göttingen: Cuvillier)
- [12] Stöber D *et al* 1987 *J. Magn. Magn. Mater.* **69** 144
- [13] Chang N C and Gruber J B 1964 *J. Chem. Phys.* **41** 3227
- [14] Takahashi M 1977 *J. Phys. C: Solid State Phys.* **10** 1289
- [15] Abragam A and Bleaney B 1970 *Electron Paramagnetic Resonance of Transition Ions* (Oxford: Clarendon)
- [16] Toulouse G 1977 *Commun. Phys.* **2** 115
- [17] Khokhlachev S B 1976 *Sov. Phys.—JETP* **43** 137
- [18] Aharony A *et al* 1998 *Dynamical Properties of Unconventional Magnetic Systems (NATO ASI Series E vol 349)* ed A T Skjeltorp and D Sherrington (Dordrecht: Kluwer)
- [19] Moessner R and Chalker J T 1998 *Phys. Rev. B* **58** 12049
- [20] Moessner R and Sondhi S L 2001 *Phys. Rev. B* **63** 224401
- [21] Harris M J *et al* 1997 *Phys. Rev. Lett.* **97** 2554
- [22] Dai D and Whangbo M H 2004 *J. Chem. Phys.* **121** 672
- [23] Harrison A 2004 *J. Phys.: Condens. Matter* **16** S553
- [24] Ciftja O *et al* 1999 *Phys. Rev. B* **60** 10122
- [25] Ciftja O 2000 *Physica A* **286** 541
- [26] Ciftja O 2001 *J. Phys. A: Math. Gen.* **34** 1611